show that hardly any commercial enhancement program can be regarded as clearly successful. Model simulations suggest, however, that stock-enhancement may be possible if releases can be made that match closely the current ecological and environmental conditions. However, this requires improvements of assessment methods of these factors beyond present knowledge. Marine systems tend to have strong nonlinear dynamics, and unless one is able to predict these dynamics over a relevant time horizon, release efforts are not likely to increase the abundance of the target population.

See also

Mariculture, Environmental, Economic and Social Impacts of. Salmonid Farming. Salmon Fisheries: Atlantic; Pacific. Salmonids.

Further Reading

Asplin L, Salvanes AGV and Kristoffersen JB (1999) Non-local wind-driven fjord–coast advection and its potential effect on pelagic organisms and fish recruitment. *Fisheries Oceanography* 8: 255–263.

Blaxter JHS (2000) The enhancement of marine fish stocks. *Advances in Marine Biology* 38: 2–54.

Coleman F, Travis J and Thistle AB (1998) *Marine Stock Enhancement: A New Perspective*. Bulletin of Marine Science 62.

Danielssen DS, Howell BR and Moksness E (1994) *An International Symposium on Sea Ranching of Cod and other Marine Fish Species. Aquaculture and Fisheries Management* 25(Suppl. 1).

Finney B, Gregory-Eaves I, Sweetman J, Douglas MSV and Smol JP (2000) Impacts of climatic change and fishing on Pacific salmon over the past 300 years. *Science* 290: 795–799.

Giske J and Salvanes AGV (1999) A model for enhancement potentials in open ecosystems. In: Howell BR, Moksness E and Svåsand T (eds) *Stock Enhancement and Sea Ranching*. Blackwell Fishing, News Books.

Howell BR, Moksness E and Svåsand T (1999) *Stock Enhancement and Sea Ranching*. Blackwell Fishing, News Books.

Kareiva P, Marvier M and McClure M (2000) Recovery and management options for spring/summer chinnook salmon in the Columbia River basin. *Science* 290: 977–979.

Mills D (1989) *Ecology and Management of Atlantic Salmon*. London: Chapman & Hall.

Ricker WE (1981) Changes in the average size and average age of Pacific salmon. *Canadian Journal of Fisheries and Aquatic Science* 38: 1636–1656.

Salvanes AGV, Aksnes DL, Fosså JH and Giske J (1995) Simulated carrying capacities of fish in Norwegian fjords. *Fisheries Oceanography* 4(1): 17–32.

Salvanes AGV, Aksnes DL and Giske J (1992) Ecosystem model for evaluating potential cod production in a west Norwegian fjord. *Marine Ecology Progress Series* 90: 9–22.

Salvanes AGV and Baliño B (1998) Production and fitness in a fjord cod population: an ecological and evolutionary approach. *Fisheries Research* 37: 143–161.

Shelbourne JE (1964) The artificial propagation of marine fish. *Advances in Marine Biology* 2: 1–76.

Svåsand T, Kristiansen TS, Pedersen T *et al.* (2000) The biological and economical basis of cod stock enhancement. *Fish and Fisheries* 1: 173–205.

Thorpe JE (1980) *Salmon Ranching*. London: Academic Press.

OCEAN SUBDUCTION

R. G. Williams, University of Liverpool, Liverpool, UK

doi:10.1006/rwos.2001.0109

Introduction

Ocean subduction involves the transfer of fluid from the mixed layer into the stratified thermocline (**Figure 1**). The upper ocean is ventilated principally through the subduction process, while the deep ocean is ventilated through open-ocean convection and cascading down coastal boundaries. The term 'ocean subduction' makes the geologicial analogy of a subduction zone where a rigid plate of the Earth's lithosphere slides beneath a more buoyant plate and into the hotter part of the mantle.

Ventilation connects the atmosphere and ocean interior through the transfer of fluid from the surface mixed layer into the ocean interior. Water masses are formed in the surface mixed layer and acquire their characteristics through the exchange of heat, moisture, and dissolved gases with the atmosphere. When the water masses are transferred beneath the mixed layer, they are shielded from the atmosphere and only subsequently modify their properties by mixing in the ocean interior. Hence, the ventilation process helps to determine the relatively long memory of the ocean interior, compared with the surface mixed layer.

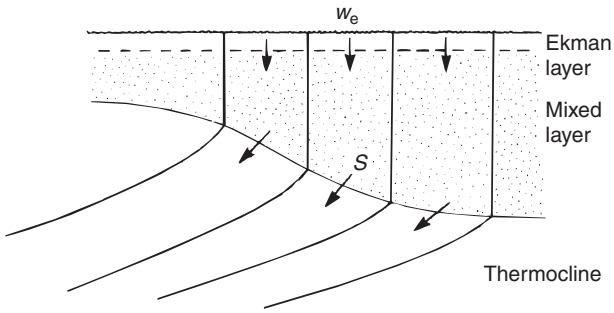

Figure 1 A schematic diagram showing isopycnals in the thermocline outcropping into a vertically homogeneous mixed layer. The subduction rate, S, measures the rate at which the stratified thermocline is ventilated through the vertical and horizontal transfer of fluid from the mixed layer. In comparison, the wind-induced, Ekman pumping, w_e, measures the vertical flux pumped down from the surface Ekman layer. (Reproduced with permission from Marshall *et al*. (1993).)

Subduction occurs throughout the ocean over recirculating wind-driven gyres within ocean basins (with horizontal scales of several thousand kilometers), across frontal zones and convective, overturning chimneys (on horizontal scales of several hundred to tens of kilometers). The reverse of the subduction process leads to the transfer of fluid from the main thermocline into the seasonal boundary layer, which affects the properties of the mixed layer and air–sea interaction.

Subduction Process

The subduction process involves the seasonal cycle of the mixed layer (**Figure 2**). The mixed layer is vertically homogenous through the action of convective overturning and turbulent mixing. At the end of winter, the mixed layer is at its maximum density and thickness, and overlies the main thermocline (where there is a strong vertical temperature gradient). During spring and summer, the surface warming forms a seasonal thermocline, which is capped by a thin, wind-stirred, mixed layer. During autumn and winter, the cooling of the surface ocean leads to a buoyancy loss and convective overturning. The mixed layer thickens and entrains fluid from the underlying thermocline until the cooling phase ceases at the end of winter.

Fluid is subducted from the mixed layer into the thermocline during the warming in spring and summer, whereas fluid is entrained into the mixed layer from the thermocline during the cooling in autumn and winter. Whether there is annual subduction of fluid into the thermocline depends on the buoyancy input into a water column. If there is a buoyancy input over an annual cycle (as depicted in **Figure 2**), the mixed layer at the end of winter becomes lighter and thinner than at the end of the previous winter. In this case, fluid is subducted into the main or permanent thermocline over the annual cycle.

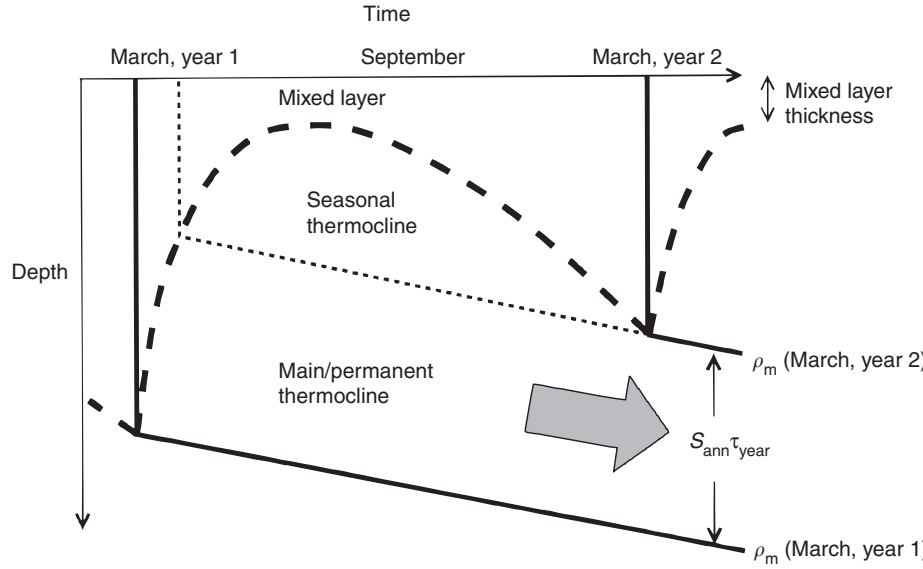

Figure 2 A schematic diagram illustrating the seasonal cycle of the mixed layer following the movement of a water column. The mixed layer thins in spring and summer, and thickens again in autumn and winter. If there is an overall buoyancy input, the end of winter mixed layer becomes lighter and thinner from one year to the next (as depicted here). Consequently, fluid is subducted irreversibly from the mixed layer into the main or permanent thermocline. The mixed layer thickness is marked by the thick dashed line, isopycnals ρ_m outcropping at the end of winter into the mixed layer by the full lines, and the isopycnal identifying the base of the seasonal thermocline by the short dashed line. The annual subduction rate, S_{ann}, determines the vertical spacing between the isopycnals subducted from the mixed layer in March for consecutive years 1 and 2 (τ_{year} is one year).

Conversely, if there is a buoyancy loss over an annual cycle, the mixed layer at the end of winter becomes denser and thicker than at the end of the previous winter. In this case, there is annual transfer of fluid from the main thermocline into the seasonal boundary layer (defined by the maximum thickness of the winter mixed layer).

Seasonal Rectification

The subduction process leads to an asymmetrical coupling between the mixed layer and main thermocline. For example, the temperature and salinity relation in the main thermocline is observed to match that of the winter mixed layer, rather than the annual average of the mixed layer. This biased coupling is due to the seasonal cycle of the mixed layer. Isopycnals in the mixed layer (density outcrops) migrate poleward in the heating seasons and retreat equatorward in the cooling seasons. This seasonal displacement of density outcrops is much greater than the movement of fluid particles over an annual cycle. Consequently, fluid subducted from the mixed layer in summer is reentrained into the mixed layer during the subsequent cooling seasons (**Figure 3**) (through the equatorial migration of density outcrops and winter thickening of the mixed layer). Fluid only succeeds in being permanently subducted into the main thermocline over a short window, one to two months long, at the end of winter when the density outcrops are at the equatorial end of their cycle. Hence, there is a seasonal rectification in the transfer of water-mass properties from the mixed layer into the ocean interior. Idealized tracer experiments suggest that the seasonal rectification still occurs even in the presence of a vibrant, time-varying circulation.

Formation of Mode Waters

There are local maxima in the subduction and ventilation processes leading to the formation of characteristic 'mode' waters, which are apparent in a volumetric census of the temperature and salinity characteristics of the ocean. These mode waters consist of large volumes of weakly stratified fluid with nearly vertically homogeneous properties. For example, strong buoyancy loss to the atmosphere over the Gulf Stream leads to the formation of 18°C mode water within the mixed layer, which is subducted following a buoyancy input along the anticyclonic circulation south of the Gulf Stream. Signals of mode water formation over the North Atlantic are revealed in diagnostics of water-mass formation from surface buoyancy fluxes, which are shown later in **Figure 11**.

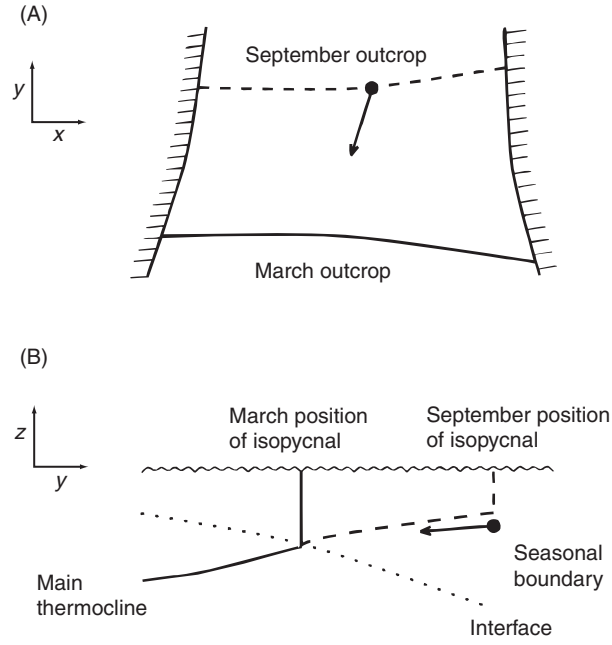

Figure 3 A schematic diagram illustrating the seasonal rectification of subduction for (A) a plan view at the sea surface and (B) a meridional section. Over the cooling season in the Northern Hemisphere, the outcrop of a density surface migrates equatorward from September to March (denoted by dashed and full lines). Consider a fluid parcel (circle) subducted from the vertically homogeneous mixed layer and advected equatorwards along this density surface. If the fluid parcel is advected past the March outcrop during the year, then it is subducted in to the main thermocline (the upper extent of which is shown by the dotted line), otherwise it is eventually entrained into the mixed layer. (Reproduced with permission from Williams *et al.* (1995).)

Definitions of Subduction Rate

The instantaneous subduction rate, S, the volume flux from the mixed layer into the stratified thermocline is given by eqn [1].

$$S = -\frac{\partial h}{\partial t} - w_{\mathrm{b}} - \mathbf{u}_{\mathrm{b}}.\nabla h \equiv -w_{\mathrm{b}} - \frac{D_{\mathrm{b}}h}{Dt} \quad [1]$$

S is defined as positive when fluid is transferred into the thermocline (**Figure 4**); h is the thickness of the mixed layer, w_{b} and $\mathbf{u}_{\mathrm{b}}$ are the vertical velocity and horizontal velocity vector, respectively, at the base of the mixed layer, and $D_{\mathrm{b}}/Dt \equiv \partial/\partial t + \mathbf{u}_{\mathrm{b}}.\nabla$ is the Lagrangian rate of change following the horizontal flow at the base of the mixed layer. The subduction rate is defined as the volume flux per unit horizontal area in [1] relative to the base of the instantaneous mixed layer. Hence, S includes a contribution from the change in thickness of the mixed layer, as well as from the vertical and horizontal movement of

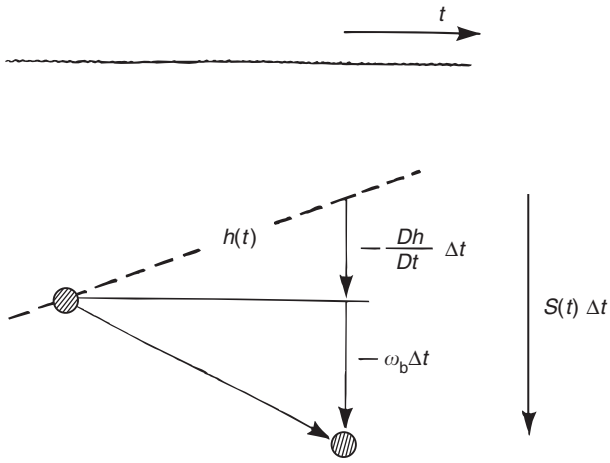

Figure 4 A schematic diagram showing a particle being subducted from the time-varying base of the mixed layer into the thermocline. The vertical distance between the particle and the mixed layer, $S(t)\Delta t$, is the sum of the vertical displacement of the particle, $-w_b\Delta t$, and the shallowing of the mixed layer following the particle, $-(Dh/Dt)\Delta t$; where h is the thickness of the mixed layer, w_b is the vertical velocity and Δt is a time interval. (Reproduced with permission from Marshall *et al.* (1993).)

fluid particles. Equivalently, S in eqn [1] can be evaluated from the vertical velocity and the Lagrangian change in mixed-layer thickness following the horizontal circulation.

The subduction into the main thermocline is physically more important than that into the seasonal thermocline, since water-mass properties become shielded from the atmosphere for longer timescales within the main thermocline. The annual rate of subduction into the main thermocline, S_{ann}, is evaluated from the volume flux per unit horizontal area passing through a control surface H that overlies the main thermocline (eqn [2]).

$$S_{ann} = -w_H - \mathbf{u}_H \,.\, \nabla H \qquad [2]$$

w_H and $\mathbf{u}_H$ are the vertical velocity and horizontal velocity vector at the depth H. The control surface is defined by the base of the seasonal thermocline given by the maximum thickness of the winter mixed layer (**Figure 1**).

Alternatively, S_{ann} may be evaluated directly from S in eqn [1] using a Lagrangian integration following the movement of a water column over an annual cycle. For example, for the mixed-layer cycle shown in **Figure 2**, S_{ann} controls the vertical spacing between isopycnals subducted at the end of consecutive winters. Hence, a high rate of subduction leads to the formation of a mode water with a weak stratification (and a large vertical spacing between subducted isopycnals).

Gyre-scale Subduction

Subduction occurs over ocean basins predominantly through the gyre-scale circulation. The surface wind-stress drives anticyclonic and cyclonic recirculations, referred to as subtropical and subpolar gyres, respectively, within a basin. The wind forcing induces downwelling of surface fluid over the subtropical gyre and upwelling over the subpolar gyre. The gyre-scale subduction rate defined in eqn [2] depends on both the vertical and horizontal circulations together with the thickness of the end of winter mixed layer.

Subduction Rate over the North Atlantic

The North Atlantic is the most actively ventilated oceanic basin. The wind-induced downwelling reaches magnitudes of $25–50\,m\,y^{-1}$ over the North Atlantic (**Figure 5A**), which is characteristic of most basins. However, the annual subduction rate is significantly enhanced over the vertical transfer through the lateral transfer across the sloping base of the mixed layer. The surface buoyancy loss to the atmosphere leads to the winter mixed layer thickening poleward, from typically 50 m in the subtropics (e.g., at 20°N) to 500 m or more in the subpolar gyre (e.g., at 50°N).

Over the subtropical gyre, the annual subduction rate reaches between $50\,m\,y^{-1}$ and $100\,m\,y^{-1}$ (**Figure 5B**). South of the Gulf Stream, there is a band of high subduction rates that are controlled by the lateral transfer. Elsewhere, the vertical and horizontal transfers are comparable over the subtropical gyre.

Over the subpolar gyre, fluid is generally transferred from the main thermocline into the seasonal boundary layer. Fluid is eventually returned from the seasonal boundary layer and into the interior through deep convection events or through subduction along the western boundary of the subpolar gyre. The negative subduction rates reach several $100\,m\,y^{-1}$ over the North Atlantic (**Figure 5B**), which is controlled by the lateral transfer rather than the vertical transfer. This negative subduction leads to water-mass properties of the main thermocline being transferred or inducted into the downstream winter mixed layer. This induction process is particularly important for the biogeochemistry in transferring inorganic nutrients from the thermocline into the winter mixed layer. These nutrients are entrained into the euphotic zone

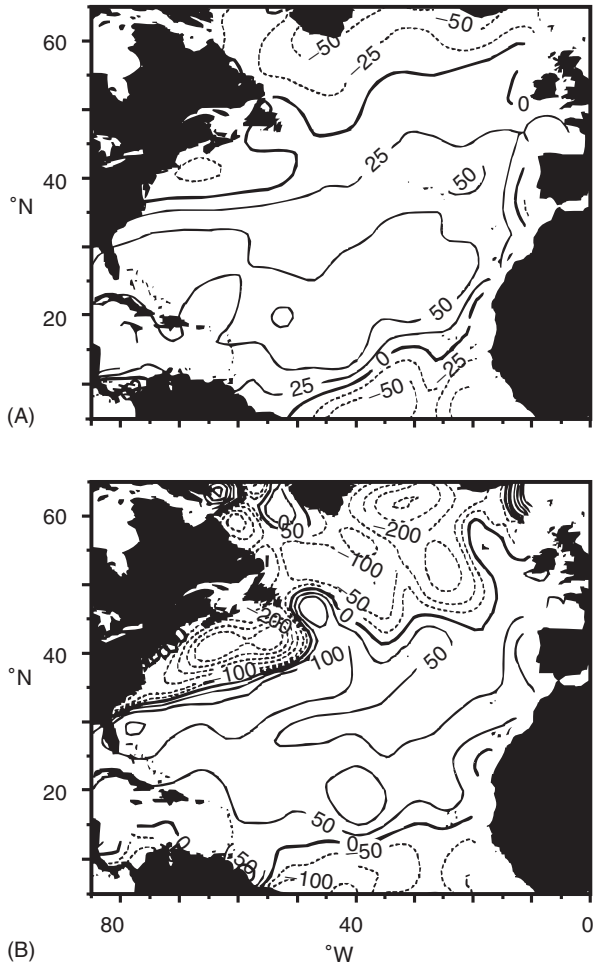

Figure 5 Diagnostics for (A) wind-driven Ekman downwelling velocity (contours every $25\,m\,y^{-1}$) and (B) annual subduction rate into the main thermocline of the North Atlantic (contours every $50\,m\,y^{-1}$). The annual subduction rate is evaluated from $S_H = -w_H - \mathbf{u}_H.\nabla H$ with the interface H defined from the mixed-layer thickness at the end of winter, $\mathbf{u}_H$ evaluated from a density climatology using thermal-wind balance, and w_H derived from the wind-stress climatology and linear vorticity balance. The subduction rate represents the volume flux per unit horizontal area which ventilates the stratified thermocline. (Reproduced with permission from Marshall *et al.* (1993).)

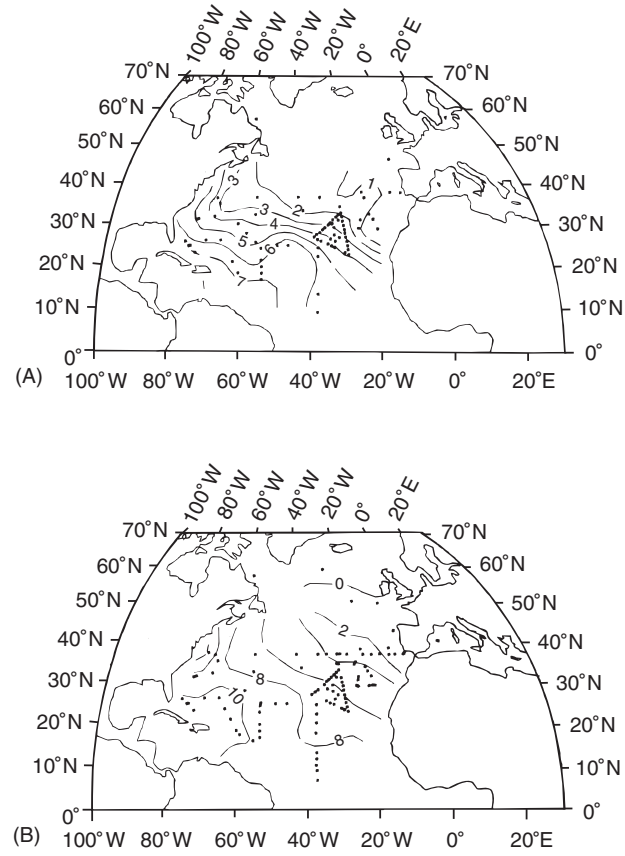

Figure 6 Observations of the tritium–helium age (years) on potential density surfaces $\sigma_\theta = 26.5$ (A) and $\sigma_\theta = 26.75$ (B) in the North Atlantic. These surfaces are ventilated from the north east and the tritium–helium age increases following the anticyclonic circulation of the subtropical gyre. (Reproduced with permission from Jenkins WJ (1988) The use of anthropogenic tritium and helium-3 to study subtropical gyre ventilation and circulation. *Philosophical Transactions of the Royal Society of London A* 325, 43–61.)

and enable high values of biological production to occur.

Evidence from Transient Tracers

Characteristic signals of subduction and ventilation are provided by distributions of transient tracers, such as tritium and CFCs (chloroflurocarbons), over the ocean interior. Quantitative information on the ventilation process is provided when the transient tracers have a known source function and lifetime. For example, in the North Atlantic, the tritium–helium age distribution along potential density surfaces reveals the general ventilation of the subtropical gyre from the north east and gradual aging following the anticyclonic circulation (**Figure 6**). The invasion of transient tracers into the main thermocline provides an integrated measure of ventilation including the contribution of the time-mean circulation and the rectified contribution of eddies. For example, the rate of ventilation inferred from the tracer age distribution is two to three times greater than the rate of wind-induced (Ekman) downwelling, which is possibly consistent with the gyre-scale subduction rate diagnostics in **Figure 5**. However, the rate of ventilation inferred from influx of tracers also includes a diffusive contribution, which differs for different tracers, making a more exact comparison with the subduction rate based on volume fluxes difficult to achieve.

Subduction and the Main Thermocline

Formation of the Main Thermocline

Throughout the ocean there is a persistent thermocline separating the mixed layer and the weakly stratified deep ocean. In ideal thermocline theory, the subduction process forms an upper thermocline over the subtropical gyre. The wind-driven circulation drives downwelling over a subtropical gyre, which leads to fluid being subducted from the mixed layer into the adiabatic interior of the ocean — see the seminal work of Luyten *et al.* (1983) listed in the Further Reading section.

The thermocline is an advective feature formed through the circulation tilting the horizontal contrast in surface density over the subtropical gyre into the vertical. The subducted thermocline extends over the mixed-layer density range within the subtropical gyre. However, observations reveal that the thermocline also extends over denser isopycnals that do not outcrop within the subtropical gyre. Thermocline models incorporating diffusion suggest that this denser thermocline may be formed through the vertical convergence of downwelling of subtropical fluid and upwelling of denser fluid originating from outside the subtropical gyre, such as from the subpolar gyre or Southern Ocean.

Dynamical Tracer Distributions

The subduction process helps to determine the stratification within the main thermocline, and hence the distribution of a dynamic tracer, the potential vorticity. Fluid parcels conserve potential vorticity for adiabatic, inviscid flow. Potential vorticity depends on the absolute spin of the fluid and stratification. A large-scale estimate of potential vorticity is provided by eqn [3] where $f = 2\Omega \sin\theta$ is the Coriolis parameter or planetary vorticity, Ω is the Earth's angular velocity, θ is the latitude, σ is a potential density and ρ is a reference density.

$$Q = -\frac{f}{\rho}\frac{\partial \sigma}{\partial z} \qquad [3]$$

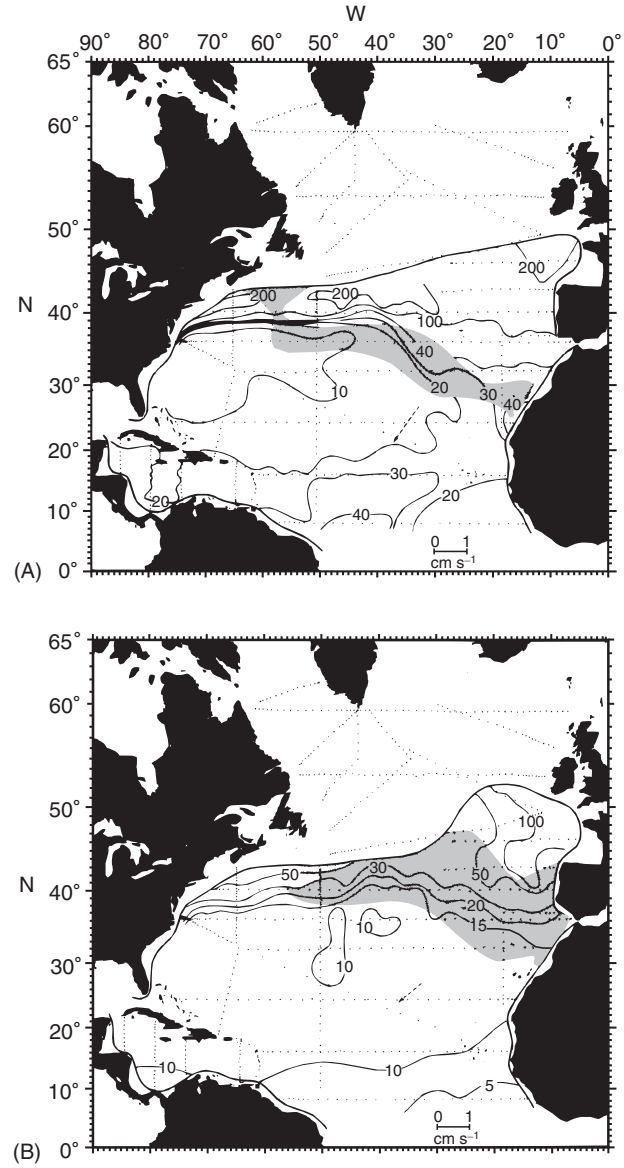

Figure 7 Diagnosed distribution of a dynamic tracer, potential vorticity Q ($10^{-11}\,m^{-1}\,s^{-1}$), over the North Atlantic. (A) Between the potential density $\sigma_\theta = 26.3$ and 26.5 surfaces, the Q contours appear to be closed in the north-west Atlantic, or to be open and thread back to the winter outcrop (shaded area) in the north-east Atlantic. (B) Between the $\sigma_\theta = 26.5$ and 27.0 surfaces, the Q field appears to be relatively homogeneous south of the winter outcrop over most of the subtropical gyre. (Reproduced with permission from McDowell *et al.* (1982).)

Climatological maps of large-scale potential vorticity over the main thermocline reveal different regimes consisting of open, closed, or blocked Q contours along potential density surfaces (**Figure 7**). The open Q contours thread from the stratified interior to the mixed-layer outcrop at the end of winter (**Figure 7A**). Conversely, closed Q contours do not intersect the mixed layer and usually contain regions of nearly uniform Q (**Figure 7B**). The blocked contours run zonally from coast to coast and are usually associated with weak meridional flow unless directly forced. The open Q contours dominate for lighter surfaces, whereas the closed or blocked Q contours dominate for denser surfaces.

Competing Paradigms: Gyre-scale Subduction versus Eddy Stirring

Different hypotheses involving gyre-scale subduction or eddy stirring have been invoked to explain these contrasting tracer distributions seen in the data.

Open tracer contours (such as in **Figure 7A**) are usually associated with gyre-scale subduction. Fluid is subducted from the end of winter mixed layer and, when the flow is adiabatic and inviscid, streamlines become coincident with Q contours in the thermocline. A thermocline model example is shown in **Figure 8**, where Q along potential density surfaces in the thermocline is determined by subduction from the overlying mixed layer. The isopleths of Q reveal the anticyclonic circulation of the subtropical gyre. The Q contrast in the thermocline can become small given realistic end of winter mixed-layer variations. In an ideal thermocline model, each potential density surface can be separated into a ventilated zone, which divides unventilated regions of a western pool and an eastern shadow zone. The unventilated zones are not directly connected by the time-mean streamlines to the overlying mixed layer, although they may still be indirectly ventilated through mixing acting along the coastal boundaries. The ventilated zone extends over most of the subtropical gyre for light potential density surfaces, but contracts eastwards for denser surfaces.

Nearly uniform tracer distributions (such as in **Figure 7B**) are instead usually associated with stirring by mesoscale eddies. The eddy stirring can homogenize conserved tracers within closed streamlines. An eddy-resolving model example is shown in **Figure 9** for a pair of wind-driven gyres. Advection by the gyre circulation leads to tracer contours and streamlines becoming nearly coincident and closed over much of the interior domain. Eddy stirring transfers tracer down-gradient within these closed contours, which forms extensive regions of nearly uniform tracer. This interpretation is supported through observations of nearly uniform distributions of tritium, as well as potential vorticity, along weakly ventilated potential density surfaces within the wind-driven gyres of the North Pacific and North Atlantic.

Gyre-scale subduction and eddy stirring are not mutually exclusive processes, and can occur simultaneously and modify each other (as revealed in general circulation model experiments). Ventilation helps control the input of tracer and the tracer contrast along the winter outcrop of the potential density surface, while eddies act to smear out subducted mode waters and tracer contrasts in the ocean interior. Diagnostics from transient tracers and float trajectories suggest that the implied Peclet number (a nondimensional measure of advection/diffusion) is typically less than 10. This value is much smaller than the high value expected from nondiffusive, ideal thermocline models. Hence, eddy diffusion appears to be significant along potential density surfaces throughout a basin and is particularly important in regions of weak background flow.

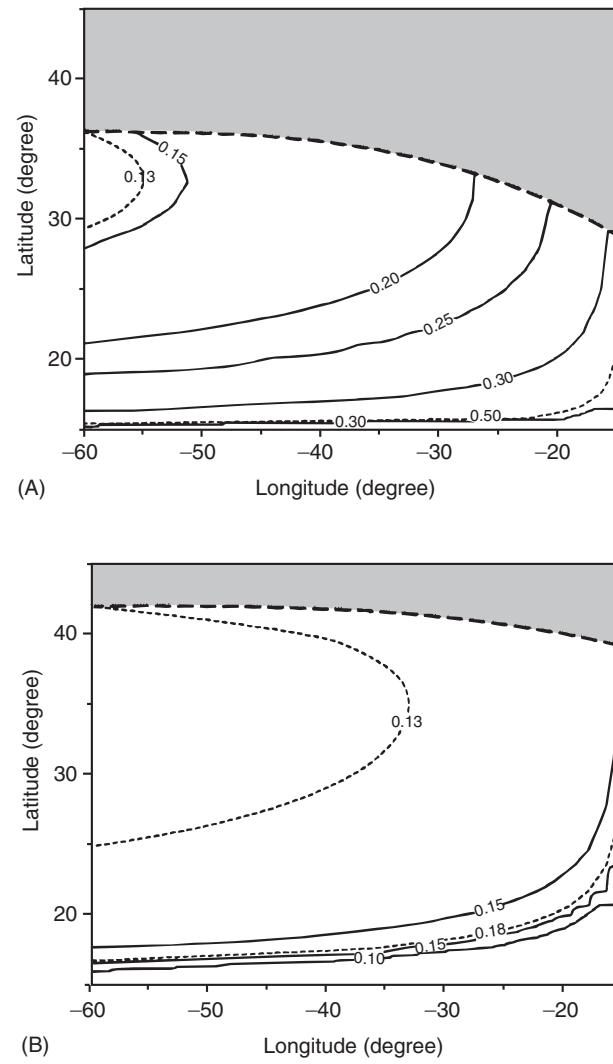

Figure 8 An ideal thermocline model solution for the dynamic tracer, potential vorticity Q ($10^{-9}\,m^{-1}\,s^{-1}$), along (A) $\sigma_\theta = 26.4$ surface and (B) the $\sigma_\theta = 26.75$ surface. Fluid is subducted across the density outcrop in the mixed layer (thick dashed line) into the stratified thermocline within a ventilated zone (between the thin dashed lines). Streamlines are coincident with the potential vorticity contours in the adiabatic interior. Given appropriate mixed-layer variations, the subducted potential vorticity can become nearly uniform, as obtained in (B). These model solutions are for an imposed anticyclonic wind forcing and a mixed layer, which becomes thicker to the north and denser to the north and east. (Reproduced with permission from Williams (1991).)

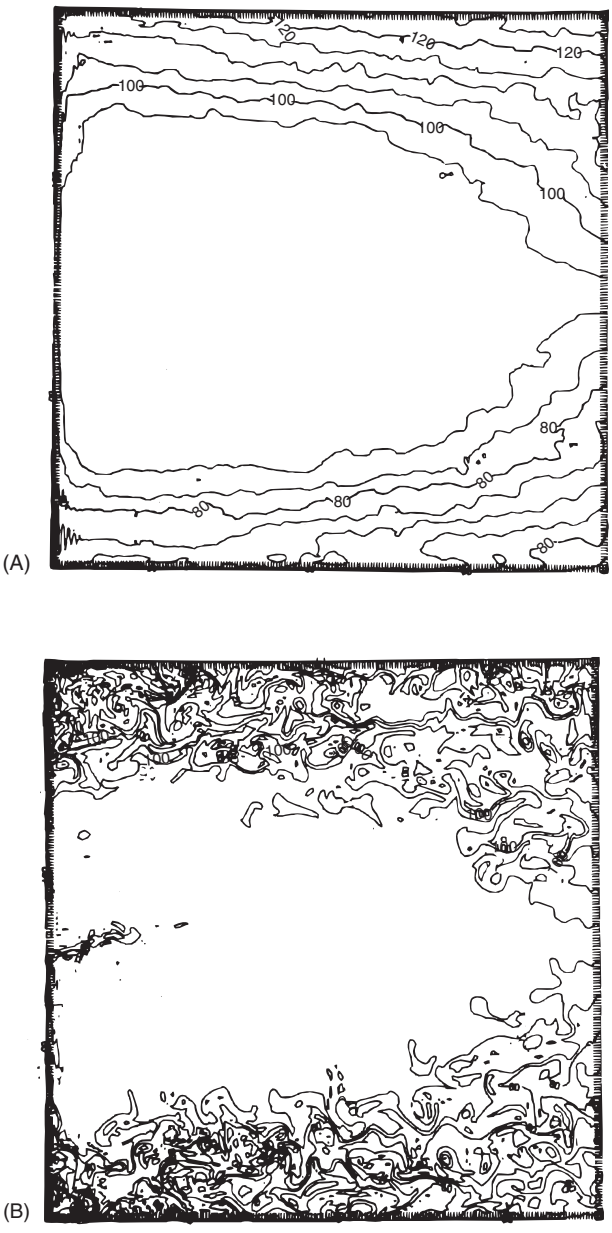

Figure 9 An eddy-resolving, three-layer model solution for the dynamic tracer, potential vorticity, for a double wind-driven gyre over a rectangular basin: plan views of (A) climatological mean and (B) instantaneous potential vorticity for the intermediate layer. The wind forcing drives a pair of wind gyres antisymmetrically about the middle latitude, which are unstable, generating a vigorous mesoscale eddy circulation. The eddy stirring leads to the time-averaged potential vorticity (in (A)) becoming nearly uniform within the circulating gyres, while outside the gyres there is a poleward increase arising from the meridional gradient in planetary vorticity. The instantaneous potential vorticity (in (B)) shows nearly perfect homogenization within the pair of gyres. At the edges of the gyre, the eddy activity is apparent through the winding up of potential vorticity contours. An experiment by W. Holland. (Reproduced from Rhines PB and Young WR (1982) Homogenization of potential vorticity in planetary gyres. *Journal of Fluid Mechanics* 122: 347–367, with permission from Cambridge University Press.)

The Relationship between Subduction, Potential Vorticity and Buoyancy Forcing

Local, kinematic connection The relationship between subduction rate, the mixed-layer evolution, and underlying potential vorticity is illustrated here. For a particle subducted from the mixed layer into the underlying thermocline (with a continuous match in potential density as depicted in **Figure 2**), the subduction rate [1] and potential vorticity [3] are kinematically related as in eqn [4].

$$Q = -\frac{f}{\rho S}\frac{D_b \sigma_m}{Dt} \qquad [4]$$

where $D_b\sigma_m/Dt$ is the Lagrangian change in mixed-layer potential density, σ_m, following the velocity $\mathbf{u}_b$ at the base of the mixed layer, which is usually taken to be a geostrophic streamline. Hence, Q in the thermocline is diagnostically related to the evolution of the mixed-layer density following the horizontal flow and the subduction rate — see **Figure 8** for an example of the resulting Q solution for an ideal thermocline model of a subtropical gyre.

Alternatively, eqn [4] can be rearranged to highlight how subduction occurs only when the mixed-layer density becomes lighter following a geostrophic streamline (eqn [5]).

$$S = -\frac{f}{\rho Q}\frac{D_b \sigma_m}{Dt} \qquad [5]$$

where $S > 0$ occurs when $D_b\sigma_m/Dt < 0$. This relation reflects how subduction relies on fluid being capped by a lighter mixed layer and hence transferred into the thermocline (**Figure 2**). For gyre-scale subduction, the required buoyancy input can be provided by an annual average of a surface buoyancy flux or a convergent Ekman flux of buoyancy; the latter contribution dominates in climatological diagnostics over the subtropical gyre of the North Atlantic (as implied from buoyancy diagnostics associated with **Figure 5**).

However, these kinematic relations [4] and [5] cease to be useful in a time-averaged limit in the presence of an active eddy circulation owing to the difficulty in defining an appropriate streamline. The Lagrangian change in mixed layer density, $D_b\sigma_m/Dt$, might even vanish following the time-mean geostrophic streamline and provide a misleading result from [5]. Instead, the role of the time-varying circulation in subduction and an integrated view of the buoyancy forcing need to be considered.

Integral connection An integral view of the ventilation process may be obtained by considering the conversion of water masses within a basin or restricted domain (**Figure 10**). Buoyancy fluxes at the sea surface and diffusive fluxes within the ocean lead to water masses being transformed from one density class to another. The convergence of this diapycnal volume flux, or water-mass transformation, defines the rate of water-mass formation within a particular density class. In the limit of no diffusive fluxes within the ocean, the rate of water-mass formation rate is equivalent to the area-integrated subduction rate over the particular density class into the main thermocline (**Figure 10**); this connection is exploited for the later example of a convective chimney in **Figure 13**.

The contribution of surface buoyancy fluxes to the rate of water-mass formation has been estimated from climatological air–sea fluxes. While there are significant errors in the air–sea fluxes, the diagnostics reveal how the buoyancy forcing and subduction process leads to the preferential formation of distinct mode waters in the North Atlantic (**Figure 11**), rather than creating similar rates of formation for all densities.

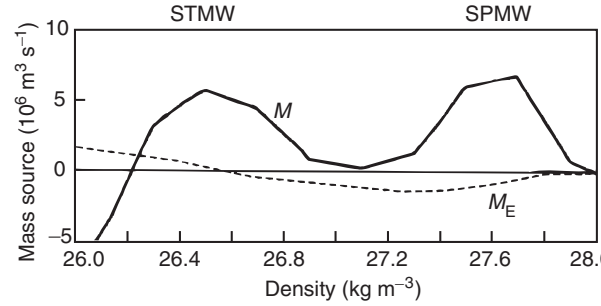

Figure 11 Diagnosed water-mass formation ($10^6\,m^3\,s^{-1}$) versus density ($kg\,m^{-3}$) evaluated from climatological surface buoyancy fluxes (full line) and from Ekman pumping (dashed line) over the North Atlantic. The left-hand peak is centered near the density of subtropical mode water (STMW) and the right-hand peak spans subpolar mode water (SPMW) and Labrador Sea Water densities. (Reproduced with permission from Speer K and Tziperman E (1992). Rates of water mass formation in the North Atlantic. *Journal of Physical Oceanography* 22: 93–104.)

Role of Eddies and Fronts

Mesoscale eddies can directly assist in the subduction process through modifying the subduction rate and diffusing the downstream properties of subducted fluid. Eddies lead to an effective stirring of water-mass properties along isopycnals. This process can lead to subducted mode waters becoming rapidly smeared out, such that the downstream water-mass properties reflect an average of the upstream characteristics determined in the mixed layer at the end of winter.

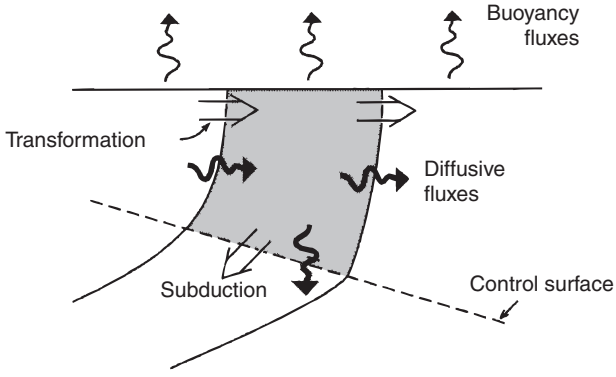

Figure 10 A schematic diagram of the upper ocean showing the sea surface, two outcropping isopycnals, and a fixed control surface across which subduction is monitored. Buoyancy fluxes at the sea surface and diffusive fluxes in the interior transform water masses from one density class to another. If there are no diffusive fluxes in the interior, the convergence of the transformation flux controls the subduction flux across the control surface (which is chosen to be the interface between the base of the end of winter mixed layer and the main thermocline). (Reproduced from Marshall J, Jamous D and Nilsson J (1999) Reconciling thermodynamic and dynamic methods of computation of water-mass transformation rates. *Deep-Sea Research I* 46: 545–572. © 1999, with permission from Elsevier Science.)

Eddy-induced Transport and Subduction

Eddies provide a volume flux and transport of tracers, which can modify the subduction rate. The eddy-driven transport, $\overline{\mathbf{u}'\Delta z'}$, is given by the temporal correlation in velocity and thickness of an isopycnal layer, Δz; the overbar represents a time average over several eddy lifetimes and the primes represent a deviation from the time average. An example of an eddy-driven transport is shown in **Figure 12A**, where the oscillating velocity leads to an eddy-driven transport through the volume flux in the thick 'blobs' of fluid being greater than the return flux in the thin 'blobs' of fluid. An eddy-induced transport velocity or 'bolus' velocity within an isopycnic layer is defined by $\mathbf{u}^* = \overline{\mathbf{u}'\Delta z'}/\overline{\Delta z}$. The eddy 'bolus' velocity is particularly large in regions of baroclinic instability, where the transport is generated through the flattening of isopycnals (**Figure 12B**).

Evaluating the instantaneous subduction rate [1] in the presence of eddies is difficult, since time-averaged correlations in velocity with mixed-layer thickness and velocity with mixed-layer outcrop area are required. However, the subduction rate into the main thermocline and across the control

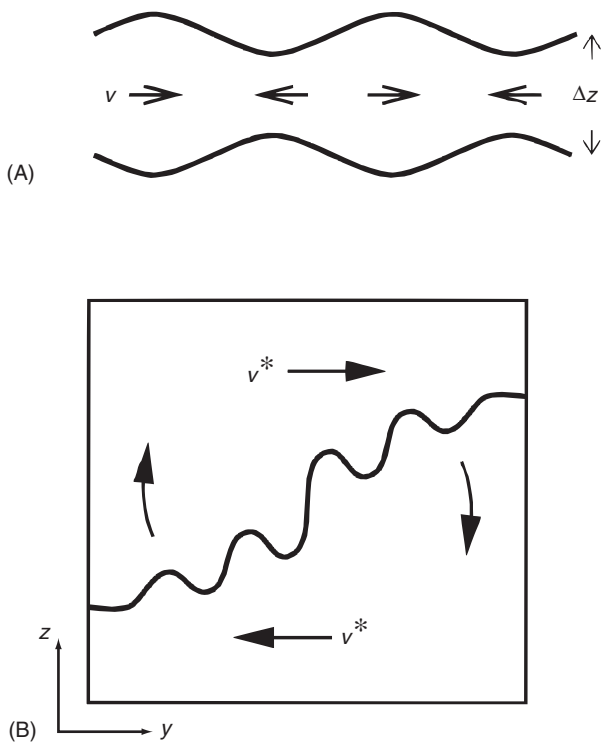

Figure 12 A schematic diagram illustrating the concept of the eddy rectified transport and 'bolus' velocity. (A) The time-averaged meridional volume flux in an undulating layer, $\overline{v\Delta z} = \bar{v}\overline{\Delta z} + \overline{v'\Delta z'}$, depends on advection by the time-mean meridional velocity $\bar{v}$ and the time-averaged correlations in the temporal deviations in velocity v' and thickness of an isopycnal layer $\Delta z'$. The time-averaged volume flux is directed to the right as drawn here, since $v > 0$ correlates with large layer thickness, while $v > 0$ correlates with small layer thickness. (B) The slumping of isopycnals in baroclinic instability induces a secondary circulation in which the bolus velocity, $v^* = \overline{v'\Delta z'}/\overline{\Delta z}$, is poleward in the upper layer and equatorward in the lower layer. Eddy-driven subduction is likely to occur in baroclinic zones where there are strongly inclined isopycnals. (Reproduced with permission from Lee M-M, Marshall DP and Williams RG (1997) On the eddy transfer of tracers: advective or diffusive? *Journal of Marine Research* 55, 483–505.)

surface, H, can be evaluated, in principle, by including the eddy-induced 'bolus' velocity in eqn [2] to give eqn [6].

$$S_{\text{ann}} = -(\bar{w}_H + w^*) - (\bar{\mathbf{u}}_H + \mathbf{u}^*).\nabla H \qquad [6]$$

The vertical eddy-transport contribution, w^*, is obtained from $\mathbf{u}^*$ through continuity. Hence, the annual subduction rate includes contributions from the time-mean and time-varying circulation. The eddy contribution to subduction is expected to be large wherever the bolus velocity is significant, such as in baroclinic zones with strongly sloping isopycnals.

Over a subtropical gyre, the subduction contribution from the time-mean circulation probably dominates over the eddy 'bolus' contribution, since the wind forcing drives an anticyclonic circulation across contours of mixed-layer thickness. However, the eddy contribution to subduction becomes crucial throughout the Southern Ocean, as well as across separated boundary currents and inter-gyre boundaries.

Subduction Associated with Fronts and Convective Chimneys

Subduction and ventilation occurs over fine scales associated with narrow fronts and convective chimneys, as well as over the larger-scale circulation. Secondary circulations develop across a front following the instability of the front and acceleration of the along stream flow. Frontal modeling studies demonstrate how this secondary circulation leads to frontal-scale subduction, which injects low stratification into the thermocline. Observational studies have identified upwelling and downwelling zones on either side of a narrow front (10 km wide) with vertical velocities reaching $40\,\text{m}\,\text{d}^{-1}$, which is much greater than the background, wind-driven, downwelling velocity. Indirect support for frontal-scale subduction is also provided by separate observations of bands of short-lived chlorophyll penetrating downward for several hundreds of meters into the stratified thermocline on the horizontal scale of 10 km; this frontal-scale process is also identified as being important in the atmosphere in transferring ozone-rich, stratospheric air into the troposphere

An example of fine-scale subduction associated with a convective chimney is shown in **Figure 13**. Buoyancy loss to the atmosphere drives the conversion of light to dense water within the mixed layer and the concomitant thickening of the mixed layer. Baroclinic instability of the chimney leads to an eddy-driven transport, which fluxes light fluid into the chimney at the surface and, in turn, subducts denser fluid into the thermocline. Hence, the eddy-driven transport enables recently ventilated dense waters to disperse away from a convective chimney. The eddy-driven influx of light fluid partly offsets the buoyancy loss to the atmosphere and can inhibit further mixed-layer deepening over the center of the chimney.

Conclusions

The subduction process controls the rate at which the upper thermocline is ventilated, as well as determining the water-mass structure and stratification of the upper ocean. Subduction leads to an

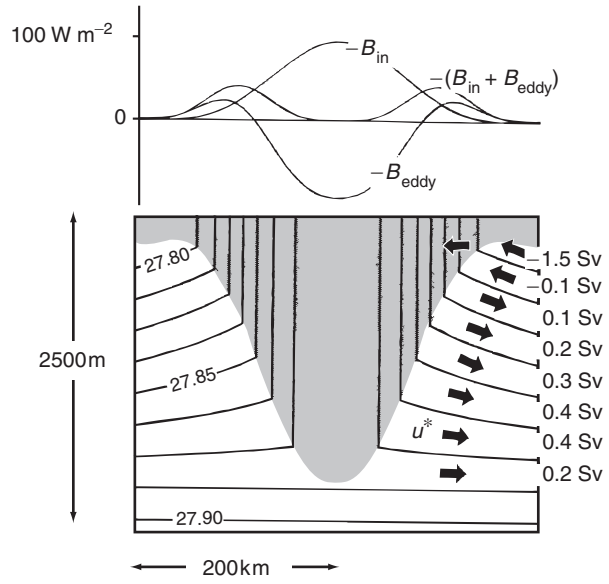

Figure 13 A model solution for the eddy-driven subduction rate and volume fluxes into and out of a convective chimney (shaded) with isopycnals depicted by solid lines. Baroclinic instability of the chimney leads to an eddy-driven circulation. There is entrainment of warm, buoyant fluid over the upper kilometer with subduction of cold, dense fluid at greater depths – the net subduction of deep water is 1.6 Sv ($1\,\mathrm{Sv} = 10^6\,\mathrm{m^3\,s^{-1}}$). The subduction rate is determined by the buoyancy forcing, $B_{in} + B_{eddy}$, where B_{in} is the surface buoyancy loss to the atmosphere and B_{eddy} is the eddy flux of buoyancy within the mixed layer. (Reproduced with permission from Marshall DP (1997).)

asymmetrical coupling between the mixed layer and ocean interior. Fluid is transferred into the permanent thermocline in late winter and early spring, rather than throughout the year. This transfer of fluid into the permanent thermocline helps to determine the relatively long memory of the ocean interior, compared with that of the surface mixed layer. Conversely, the reverse of the subduction process is also important. The induction of thermocline fluid into the seasonal boundary layer affects the downstream water-mass properties of the mixed layer, and hence alters the air–sea interaction and biogeochemistry. For example, biological production is enhanced wherever nutrients are vertically and laterally fluxed from the thermocline into the mixed layer and the euphotic zone.

Subduction can occur over a range of scales extending over fronts, meoscale eddies, and gyres. A major challenge is to identify the relative importance of the frontal, eddy, and gyre contributions to subduction. Reliable estimates of subduction rate are difficult to achieve owing to the spatial and temporal variability in the circulation and thickness of the mixed layer and the difficulty in estimating the eddy transport contributions. An additional challenge is to determine the role that subduction plays in climate variability, particularly how subduction communicates atmospheric variability to the ocean interior.

Glossary

Ventilation The transfer of fluid from the mixed layer into the ocean interior.

Subduction The transfer of fluid from the mixed layer into the stratified thermocline.

Subduction rate The volume flux per unit horizontal area passing from the mixed layer into the stratified thermocline.

Thermocline A region of enhanced vertical temperature gradient over the upper 1 km of the ocean.

Seasonal boundary layer A region over which the mixed layer and seasonal thermocline occur. The base of the seasonal boundary layer is defined by the maximum thickness of the winter mixed layer.

Potential vorticity A dynamical tracer, conserved by fluid in adiabatic and inviscid flow, which is determined by the absolute spin of the fluid and the stratification.

Sverdrup $1\,\mathrm{Sv} = 10^6\,\mathrm{m^3\,s^{-1}}$.

See also

Deep Convection. Ekman Transport and Pumping. Mesoscale Eddies. Open Ocean Convection. Overflows and Cascades. Thermohaline Circulation. Upper Ocean Mixing Processes. Upper Ocean Vertical Structure. Water Types and Water Masses. Wind and Buoyancy-forced Upper Ocean. Wind Driven Circulation.

Further Reading

Cox MD (1985) An eddy-resolving model of the ventilated thermocline. *Journal of Physical Oceanography*, 15: 1312–1324.

Cushman-Roisin B (1987) *Dynamics of the Oceanic Surface Mixed-Layer*. Hawaii Institute of Geophysical Special Publications, Muller P and Henderson D (eds), pp. 181–196.

Jenkins WJ (1987) ^{3}H and ^{3}He in the Beta triangle: observations of gyre ventilation and oxygen utilization rates. *Journal of Physical Oceanography* 17: 763–783.

Luyten JR, Pedlosky J and Stommel H (1983) The ventilated thermocline. *Journal of Physical Oceanography* 13: 292–309.

Marshall DP (1997) Subduction of water masses in an eddying ocean. *Journal of Marine Research* 55: 201–222.

Marshall JC, Nurser AJG and Williams RG (1993). Inferring the subduction rate and period over the North Atlantic. *Journal of Physical Oceanography* 23: 1315–1329.

McDowell S, Rhines PB and Keffer T (1982) North Atlantic potential vorticity and its relation to the general circulation. *Journal of Physical Oceanography* 12: 1417–1436.

Pedlosky J (1996) *Ocean Circulation Theory*. New York: Springer.

Pollard RT and Regier LA (1992) Vorticity and vertical circulation at an ocean front. *Journal of Physical Oceanography* 22: 609–625.

Price JF (2001) Subduction. In: *Ocean Circulation and Climate: Observing and Modelling the Global Ocean*, G. Siedler, J. Church and J. Gould (eds), Academic Press, pp. 357–371.

Rhines PB and Schopp R (1991) The wind-driven circulation: quasi-geostrophic simulations and theory for nonsymmetric winds. *Journal of Physical Oceanography* 21: 1438–1469.

Samelson RM and Vallis GK (1997) Large-scale circulation with small diapycnal diffusion: the two-thermocline limit. *Journal of Marine Research* 55: 223–275.

Stommel H (1979) Determination of watermass properties of water pumped down from the Ekman layer to the geostrophic flow below. *Proceedings of the National Academy of Sciences of the USA* 76: 3051–3055.

Williams RG (1991) The role of the mixed layer in setting the potential vorticity of the main thermocline. *Journal of Physical Oceanography* 21: 1803–1814.

Williams RG, Spall MA and Marshall JC (1995) Does Stommel's mixed-layer 'Demon' work? *Journal of Physical Oceanography* 25: 3089–3102.

Woods JD and Barkmann W (1986) A Lagrangian mixed layer model of Atlantic 18°C water formation. *Nature* 319: 574–576.

OCEAN THERMAL ENERGY CONVERSION (OTEC)

S. M. Masutani and P. K. Takahashi,
University of Hawaii at Manoa, Honolulu, HI, USA

doi:10.1006/rwos.2001.0031

Ocean thermal energy conversion (OTEC) generates electricity indirectly from solar energy by harnessing the temperature difference between the sun-warmed surface of tropical oceans and the colder deep waters. A significant fraction of solar radiation incident on the ocean is retained by seawater in tropical regions, resulting in average year-round surface temperatures of about 28°C. Deep, cold water, meanwhile, forms at higher latitudes and descends to flow along the seafloor toward the equator. The warm surface layer, which extends to depths of about 100–200 m, is separated from the deep cold water by a thermocline. The temperature difference, ΔT, between the surface and thousand-meter depth ranges from 10 to 25°C, with larger differences occurring in equatorial and tropical waters, as depicted in **Figure 1**. ΔT establishes the limits of the performance of OTEC power cycles; the rule-of-thumb is that a differential of about 20°C is necessary to sustain viable operation of an OTEC facility.

Since OTEC exploits renewable solar energy, recurring costs to generate electrical power are minimal. However, the fixed or capital costs of OTEC systems per kilowatt of generating capacity are very high because large pipelines and heat exchangers are needed to produce relatively modest amounts of electricity. These high fixed costs dominate the economics of OTEC to the extent that it currently cannot compete with conventional power systems, except in limited niche markets. Considerable effort has been expended over the past two decades to develop OTEC by-products, such as fresh water, air conditioning, and mariculture, that could offset the cost penalty of electricity generation.

State of the Technology

OTEC power systems operate as cyclic heat engines. They receive thermal energy through heat transfer from surface sea water warmed by the sun, and transform a portion of this energy to electrical power. The Second Law of Thermodynamics precludes the complete conversion of thermal energy in to electricity. A portion of the heat extracted from the warm sea water must be rejected to a colder thermal sink. The thermal sink employed by OTEC systems is sea water drawn from the ocean depths by means of a submerged pipeline. A steady-state control volume energy analysis yields the result that net electrical power produced by the engine must equal the difference between the rates of heat transfer from the warm surface water and to the cold deep water. The limiting (i.e., maximum) theoretical Carnot energy conversion efficiency of a cyclic heat